


Petrogenesis and tectonic implications of Triassic A-type granites in southeastern China: insights from zircon U–Pb–Hf isotopic and whole-rock geochemical compositions of the Luoguyan and Guiyantou granites in northwestern Fujian Province

Wanli Gao, Zongxiu Wang, Leilei Li & Yuanlong Tan

To cite this article: Wanli Gao, Zongxiu Wang, Leilei Li & Yuanlong Tan (2018): Petrogenesis and tectonic implications of Triassic A-type granites in southeastern China: insights from zircon U–Pb–Hf isotopic and whole-rock geochemical compositions of the Luoguyan and Guiyantou granites in northwestern Fujian Province, International Geology Review, DOI: [10.1080/00206814.2017.1422444](https://doi.org/10.1080/00206814.2017.1422444)

To link to this article: <https://doi.org/10.1080/00206814.2017.1422444>

 View supplementary material [↗](#)

 Published online: 08 Jan 2018.

 Submit your article to this journal [↗](#)

 Article views: 6

 View related articles [↗](#)

 View Crossmark data [↗](#)

ARTICLE



Petrogenesis and tectonic implications of Triassic A-type granites in southeastern China: insights from zircon U–Pb–Hf isotopic and whole-rock geochemical compositions of the Luoguyan and Guiyantou granites in northwestern Fujian Province

Wanli Gao^a, Zongxiu Wang^a, Leilei Li^{a,b} and Yuanlong Tan^a

^aKey Lab of Shale Oil and Gas Geological Survey, Institute of Geomechanics, Chinese Academy of Geological Science, Beijing, PR China;

^bSchool of Earth Science and Resources, China University of Geoscience, Beijing, PR China

ABSTRACT

Triassic A-type granites in eastern South China Block (SCB) are abundant in the Wuyi–Yunkai tectonic domain and provide an important opportunity to explore the early Mesozoic evolution of continental crust of the SE part of the SCB. We carried out U–Pb zircon dating, Lu–Hf isotope analyses of zircon, and whole-rock geochemical analyses for two granitic plutons, the Guiyantou (GYT) and Luoguyan (LGY) granites, from northwestern Fujian Province. LA–ICP–MS U–Pb zircon analyses yielded ages of 232 ± 4 to 231 ± 7 Ma and 221 ± 5 Ma (Middle–Late Triassic) for the GYT and LGY granites. These two granites belong to metaluminous to weakly peraluminous high K calc-alkaline A-type granite that are enriched in K, Al, light rare earth element and Rb, Th, U, and Pb, and depleted in Nb, Ta, P, and Ti. Their rare earth element patterns are highly fractionated with $(La/Yb)_N$ ratios of 2–21 and strong negative Eu anomalies ($Eu/Eu^* = 0.02–0.31$). *In situ* Hf isotopic analysis of zircon from the GYT and LGY granites yielded $\varepsilon_{Hf}(t)$ values ranging from –11.5 to –1.1, with corresponding two-stage Hf model ages from 1.98 to 1.33 Ga, from which it is inferred that the GYT and LGY magmas formed by partial melting of Proterozoic metasedimentary rock in the Cathaysia block. The two granites were emplaced at 232 and 221 Ma and together with Triassic A-type granites in coastal region of the SCB, which is in agreement with an extensional tectonic setting in the Middle–Late Triassic. We suggest that the Middle–Late Triassic A-type granites in eastern SCB were probably formed in an intracontinental, post-orogenic extensional regime that collision was between the SCB and an ‘unknown block’ or the eastern extension of Indochina block.

ARTICLE HISTORY

Received 3 September 2017
Accepted 26 December 2017

KEYWORDS

Triassic granites; geochronology; geochemistry; tectonic implications; South China Block


1. Introduction

The South China Block (SCB) is located in SE Asian and was formed by five tectonic events, including Neoproterozoic Jiangnan collision (Li *et al.* 2008; Yao *et al.* 2015), Late Neoproterozoic–Early Paleozoic Nanhua rifting (Shu *et al.* 2011), Early Paleozoic intracontinental orogeny (Faure *et al.* 2009; Charvet *et al.* 2010; Shu *et al.* 2015), Early–Middle Triassic intracontinental orogeny (Chu *et al.* 2012a; Wang *et al.* 2013a; Faure *et al.* 2016, 2017), and Cretaceous extension (Li 2000; Li *et al.* 2013). The Triassic appears as the most important period for the tectonic development of the SCB (Zhang *et al.* 2013; Zheng *et al.* 2013; Faure *et al.* 2016). Along with this history of collision and accretion, the SCB experienced pronounced tectonothermal activity, which created a large number of granites and ore deposits. Many valuable studies have been carried out

to explore their origin (Li and Li 2007; Sun *et al.* 2007, 2012; Wang *et al.* 2011). Triassic magmatism in the eastern SCB and its role in continental assembly has always been the focus of these studies.

Previous work suggested that the Triassic granites are all I- and S-type, and crop out far from continental margins within the central SCB (i.e. in Jiangxi, Hunan, Guangxi, and Guangdong provinces) (Zhou *et al.* 2006; Zhang *et al.* 2013; Wang *et al.* 2013a). The granites were thought to have formed in a compressional tectonic setting related to collision between the SCB and the Indochina Block (Wang *et al.* 2002, 2005a, 2007a; Zhou *et al.* 2006). In recent years, Triassic magmatism has been reported in eastern SCB (Zhejiang and Fujian provinces); this magmatism comprises A-type granites and alkaline syenites in contrast to the I- and S-type granites in the central SCB (Wang *et al.* 2005b; Sun *et al.*

CONTACT Zongxiu Wang  wangzongxiu@sohu.com  Key Lab of Shale Oil and Gas Geological Survey, Institute of Geomechanics, Chinese Academy of Geological Science, Beijing 100081, PR China

 Supplemental data for this article can be accessed [here](#).

© 2018 Informa UK Limited, trading as Taylor & Francis Group

2011; Li *et al.* 2012a; Zhao *et al.* 2013; Gao *et al.* 2014; Zhu *et al.* 2016). It has often been argued that A-type granites form in attenuated continental crust in extensional tectonic regimes (Dall'Agnol *et al.* 2012) and have been regarded as a reliable indicator of tectonic setting (Eby 1990; Förster *et al.* 1997). Some studies consider that the Triassic A-type granites in Zhejiang and Fujian provinces formed in an extensional environment after collision between the SCB and the Indochina Block (Sun *et al.* 2011; Li *et al.* 2012a; Zhao *et al.* 2013). However, others have suggested that a compressional regime was still dominant in the SCB in the Triassic, and that Early Mesozoic A-type granitoids in the eastern SCB are related to water-deficient and reduced melting conditions rather than an anorogenic tectonic setting (Zhu *et al.* 2013, 2016). The petrogenesis and tectonic setting of Triassic granites in the Cathaysia block is the subject of ongoing debate.

In this article, we present new detailed LA-ICP-MS zircon U–Pb dating, major and trace element geochemistry, and Lu–Hf isotopic data for two Triassic A-type

granites in northwestern Fujian Province to explore the petrogenesis of these A-type granites and their relationship to the early Mesozoic orogeny in the SCB (Figure 1 and Table 1).

2. Geological setting and local geology

The SCB in southeast China (Figure 1) consists of two major Precambrian continental blocks: the Yangtze block to the northwest and the Cathaysia block to the southeast (Zheng *et al.* 2008; Zhang and Zheng 2013). The two blocks were considered to have collided along the Jiangnan orogeny in the Neoproterozoic (Zhao and Cawood 2012; Wang *et al.* 2014; Yao *et al.* 2014, 2015). Basement to the Yangtze block consists of Archean rocks with average ages of 2.8–2.7 Ga (Zhang and Zheng 2013; Guo *et al.* 2015), whereas the Cathaysia block appears to be much younger and consists predominantly of Paleoproterozoic basement with several late Archean (~2.5 Ga) inliers (Xu *et al.* 2007). The Jiangshan–Shaoxing Fault marks the western boundary

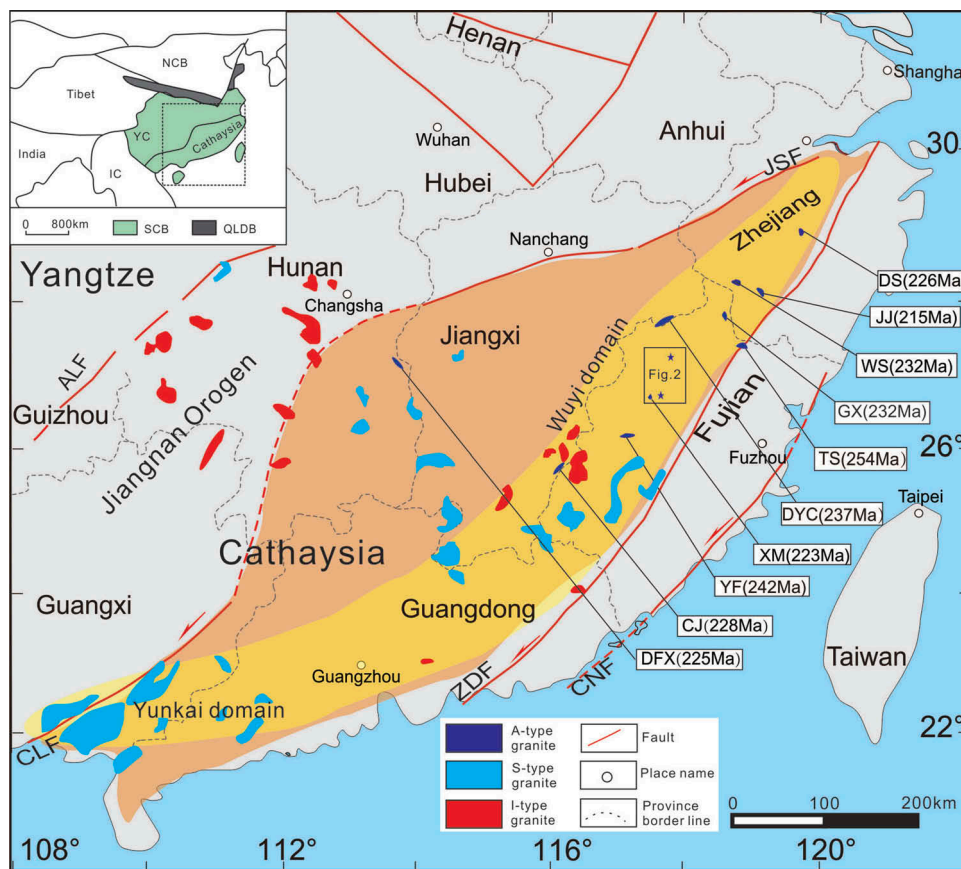


Figure 1. Map of the Triassic granite distribution, modified after (Sun *et al.* 2011). The locations and ages of Triassic A-type granites are from previous studies (DaShuang, JingJu, WengShan, GaoXi, TieShan, DaYinChang, YangFang, CaiJiang, DengFuXian), as tabulated in Table 1. The flesh-coloured and yellow regions, respectively, represent Cathaysia Block and Wuyi-Yunkai tectonic domain.

NCB: North China Block; YC: Yangtze Block; IC: Indo-China; QLDB: Qinling-Dabie; JSF: Jiangshan–Shaoxing Fault; CNF: Changle–Nanao Fault; ZDF: Zhenghe–Dafu Fault; CLF: Chenzhou–Linwu Fault; ALF: Anhua–Luocheng Fault.

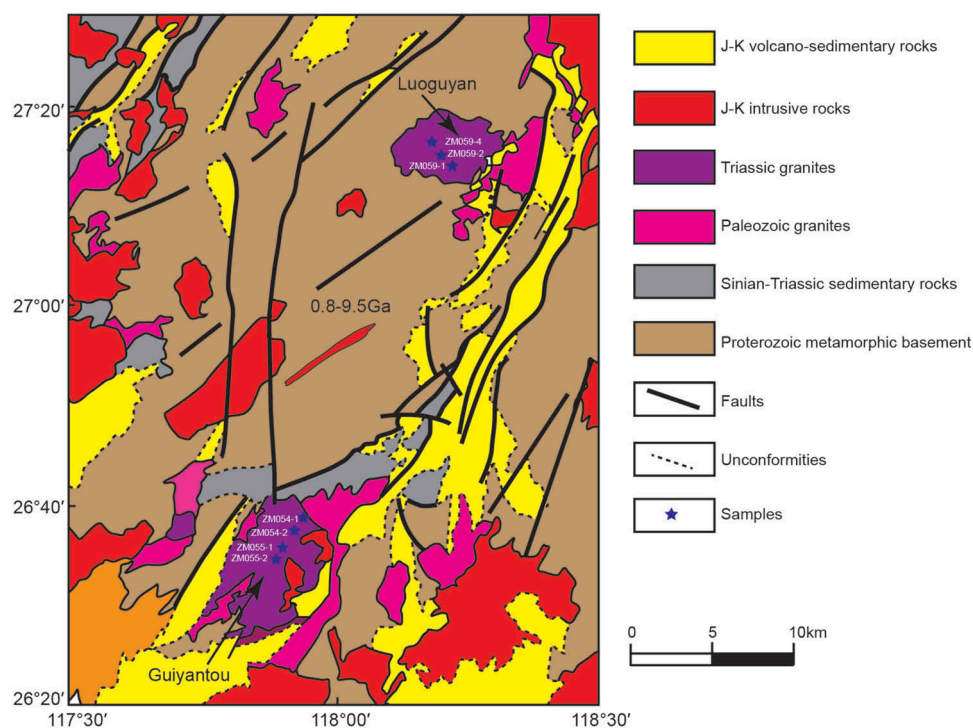
Table 1. Compiled list of the Triassic A-type granites in SE China.

No	Sample	Location	Lithology	Methods	Age (Ma)	References
1	DS	Zhejiang	Quartz-monzonite	LA-ICP-MS	234 ± 3	Gao <i>et al.</i> (2014)
			Monzogranite	LA-ICP-MS	231 ± 3	
			Quartz monzonite	LA-MC-ICP-MS	231.60 ± 0.86	Mao <i>et al.</i> (2013)
2	JJ	Zhejiang	Quartz syenite	LA-MC-ICP-MS	231.7 ± 1.1	Li <i>et al.</i> (2012a)
			Syenogranites	LA-ICP-MS	215 ± 2	
			Monzogranite	LA-ICP-MS	246 ± 2	Gao <i>et al.</i> (2014)
3	WS	Zhejiang	K-feldspar granite	LA-ICP-MS	241 ± 3	Sun <i>et al.</i> (2011)
			Monzogranites	SHRIMP	225 ± 1	
			Monzogranites	LA-ICP-MS	224 ± 3	
4	GX	Fujian	Biotite granite	LA-ICP-MS	232 ± 2	Zhao <i>et al.</i> (2013)
5	TS	Fujian	Alkaline syenite	LA-ICP-MS	254 ± 4	Wang <i>et al.</i> (2005b)
6	YF	Fujian	Alkaline syenite	LA-ICP-MS	242 ± 4	Wang <i>et al.</i> (2013b)
7	DYC	Fujian	Biotite granite	LA-ICP-MS	228 ± 2	
8	LGY	Fujian	Syenogranites	LA-ICP-MS	221 ± 5	This paper
9	GYT	Fujian	Syenogranites	LA-ICP-MS	232 ± 4	Zhao <i>et al.</i> (2013)
10	CJ	Jiangxi	Monzogranites	LA-ICP-MS	228 ± 2	
11	DFX	Hunan	Biotite granite	LA-ICP-MS	225.7 ± 1.6	Cai <i>et al.</i> (2015)

of the Cathaysia block. The NE–SW-trending Zhenghe–Dapu Fault is present in the Cathaysia block (Wang *et al.* 2013a). There are very abundant occurrences of Mesozoic magmatic rocks in the SCB, particularly in the Cathaysia block (Zhou *et al.* 2006). The early Mesozoic (Triassic) granites occur mainly between Anhua–Luocheng Faults in the west and ZDF in the east (Figure 1).

The study area is located in northern part of Fujian Province within the northeastern Cathaysia block (Figure 2). In the study area, almost all of the strata comprising the cover strike ENE. Ductile shear zones are extensively distributed through the Proterozoic basement,

which mainly comprises gneiss, mica schist, phyllite, and siliceous rock, the protoliths to which were dated as Proterozoic. The Sinian–Triassic strata consist of coarse clastic rock, volcanoclastic rock, and a carbonate assemblage. Silurian strata are absent in this region. The Jurassic–Cretaceous strata are mainly composed of a continental coal-bearing assemblage and a volcanic–sedimentary rock assemblage dated at 160–120 Ma. Three major episodes of granitic magma emplacement have been identified in the northwest Fujian Province: early Paleozoic, Triassic, and Jurassic–Cretaceous. The Early Paleozoic and Jurassic–Cretaceous intrusive rocks occupy a larger area than the Triassic granites.

**Figure 2.** Geological map of the northwestern Fujian province.

The Luoguyan and Guiyantou granitic plutons in northwestern Fujian Province are located at the eastern margin of the Wuyi domain (Figure 1). The Guiyantou granite intruded Precambrian strata (southern pluton in Figure 2) and was covered by late Paleozoic and Mesozoic strata and intruded by Jurassic-Cretaceous granites (Figure 2). The Guiyantou granite includes phases classified as syeno-granite (ZM054) and monzogranite (ZM055) in a quartz–alkalifeldspar–plagioclase–feldspathoid (QAPF) diagram (Figure 3; Streckeisen 1976), of which syeno-granite (ZM054) comprises K-feldspar (35–50%), plagioclase (10%), quartz (25–35%), and biotite (5–8%), and is medium-grained and massive (Figure 4(a,b)). The monzonite (ZM055) comprises plagioclase (35–40%), biotite (5%), K-feldspar (30–35%), and quartz (~25%) with a medium-grained hypidiomorphic–granular texture (Figure 4(c,d)). Accessory minerals include titanite, zircon, and apatite. Feldspars are partially altered to sericite, and biotite is locally altered to chlorite.

The Luoguyan granite also intruded into Precambrian strata (northern pluton in Figure 2) during the early Mesozoic. It is mainly composed of silicic-intermediate rocks (K-feldspar granite, biotite granite, and monzonite) (Figure 2). The granite (ZM059) comprises K-feldspar (40–45%), quartz (35%), plagioclase (5–10%), and amphibole (5%), with a medium-grained granitic texture (Figure 4(e,f)), which was classified as syeno-granite (ZM059) in a QAPF diagram (Figure 3). Accessory minerals include titanite, apatite, and zircon.

3. Analytical methods

Zircon grains were separated from the three samples, GYT (ZM054-1 and ZM055-1) and LGY(ZM059-1), using

standard heavy liquid and magnetic techniques before being handpicked under a binocular microscope, mounted in epoxy, and ground to approximately half their thickness. The internal textures of the grains were imaged by cathodoluminescence (CL) using an FEI PHILIPS XL30 SFEI instrument with a two-minute scan time under conditions of 15 kV and 120 nA. The Th, U, and Pb isotopic analyses of zircon were performed by laser ablation multicollector inductively coupled plasma mass spectrometry (LA-MC-ICPMS) at the Institute of Mineral Resources, Chinese Academy of Geological Sciences, Beijing, China. For details on the instrument settings and analytical procedures, see Hou *et al.* (2009). The raw ICP-MS data were processed using the ICP-MS Datacal program (Liu *et al.* 2008). Common Pb was corrected following Andersen (2002). Age calculations and plotting of concordia diagrams were performed using Isoplot (Ludwig 2001).

In situ zircon Hf isotope analyses were performed using a New-Wave UP 213 laser ablation microprobe attached to a Neptune multi-collector ICP-MS at the Institute of Mineral Resources, Chinese Academy of Geological Sciences, Tianjin. For details on the instrument conditions and data acquisition, see Hou *et al.* (2007). A stationary spot with a beam diameter of 55 μm was used for the analyses. Helium was used as the carrier gas to transport the ablated sample from the laser ablation cell to the ICP-MS torch via a mixing chamber where it was mixed with argon. To correct for instrumental mass bias, Yb isotope ratios were normalized to a $^{172}\text{Yb}/^{173}\text{Yb}$ ratio of 1.35274 (Chu *et al.* 2002) and Hf isotope ratios were normalized to a $^{179}\text{Hf}/^{177}\text{Hf}$ ratio of 0.7325 using an exponential law. The mass bias behaviour of Lu was assumed to follow that of Yb, and the mass bias correction protocol of Hou *et al.*

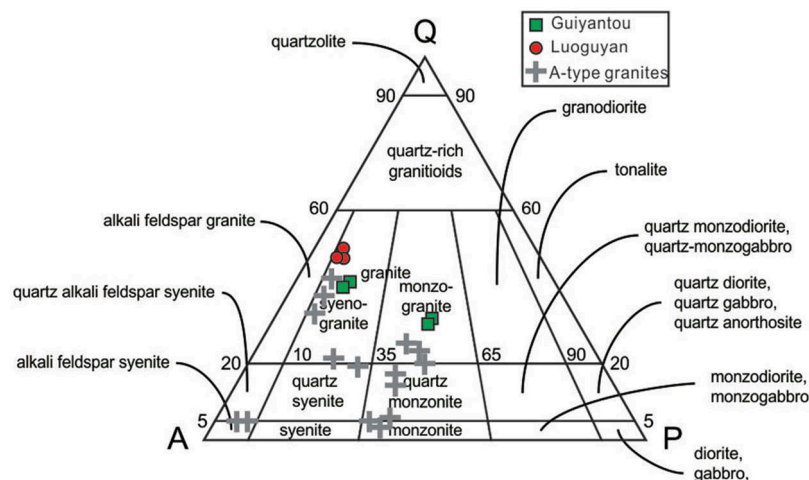


Figure 3. Nomenclature and classification system used to classify granitic rocks by mineralogy, based on the quartz–alkali feldspar–plagioclase–feldspathoid classification diagram of Streckeisen (1976). The Triassic A-type granites are from previous studies (DaShuang, JingJu, WengShan, GaoXi, TieShan, DaYinChang, YangFang, CaiJiang, DengFuXian), as tabulated in Table 1.

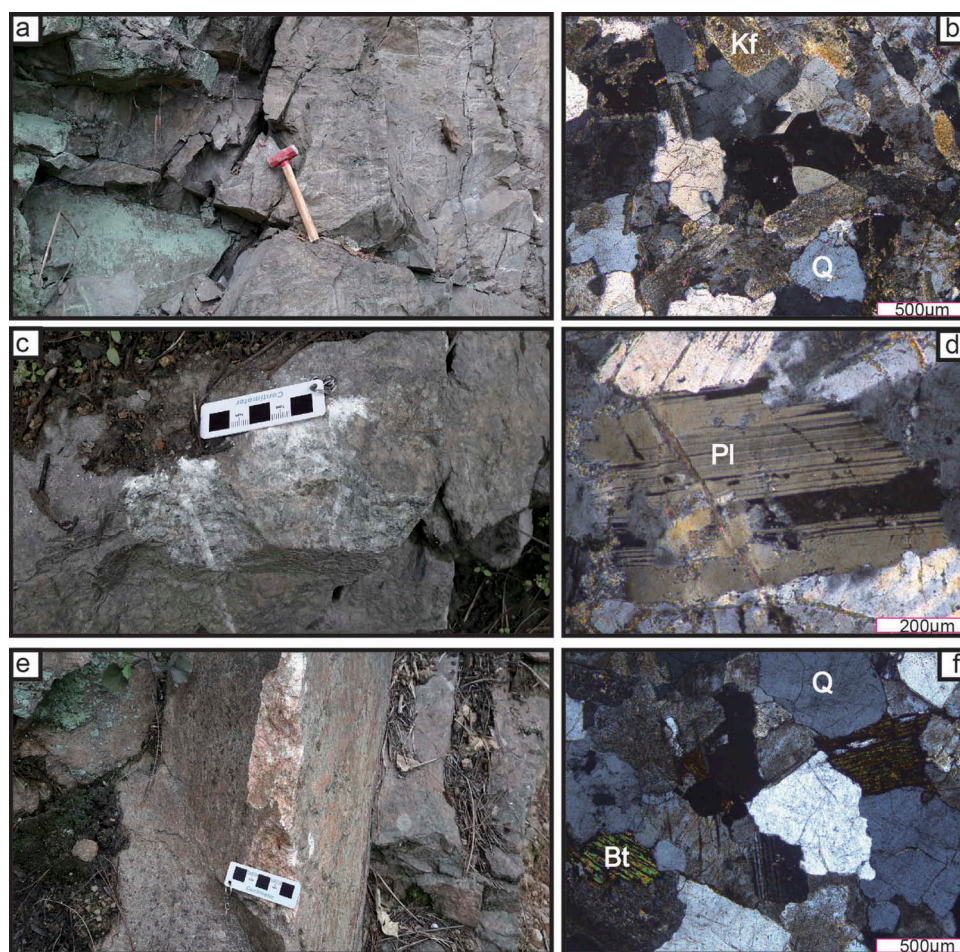


Figure 4. Field photographs and photomicrographs of the Guiyantou and Luoguyan granites. (a) Field photograph of the Guiyantou K-feldspar granite (sample ZM054). (b) Photomicrograph of the Guiyantou K-feldspar granite under cross-polarized light. (c) Field photograph of the Guiyantou monzogranite (sample ZM055). (d) Photomicrograph of the Guiyantou monzogranite under cross-polarized light. (e) Field photograph of the Luoguyan K-feldspar granite (sample ZM059). (f) Photomicrograph of the Luoguyan K-feldspar granite under cross-polarized light. Bt = biotite, Qz = quartz, Pl = plagioclase, Kf = K-feldspar.

(2007) was employed. Zircon GJ-1 was used as the reference standard with a weighted mean $^{176}\text{Hf}/^{177}\text{Hf}$ ratio of 0.282008 ± 0.000018 (2σ , $n = 34$) during our routine analyses. To calculate model ages and $\epsilon\text{Hf}(t)$ values, we adopted a depleted-mantle model with $^{176}\text{Hf}/^{177}\text{Hf} = 0.28325$ and $^{176}\text{Lu}/^{177}\text{Hf} = 0.0384$ (Griffin *et al.* 2002), and a chondritic model with $^{176}\text{Hf}/^{177}\text{Hf} = 0.282772$ and $^{176}\text{Lu}/^{177}\text{Hf} = 0.0332$ (Blichert-Toft and Albarède 1997). The decay constant of ^{176}Lu adopted for this study was $1.865 \times 10^{-11} \text{ a}^{-1}$ (Scherer *et al.* 2001). The mean crustal $^{176}\text{Lu}/^{177}\text{Hf}$ value of 0.015 was used to calculate the two-stage model ages (T_{DM}^{C}) (Griffin *et al.* 2002).

The samples for whole-rock chemical analysis were crushed to 200-mesh using an agate mill. Whole-rock chemical analyses were conducted at the National Research Center of Geoanalysis, Chinese Academy of Geological Sciences, Beijing. Major-element compositions of samples were measured by X-ray fluorescence

spectrometer (Shimadzu XRF-1800) in GPMR. The Chinese National standards GSR-3 and GRS-7 were used to monitor the data quality, and the analytical uncertainties were generally within 0.1–1% (RSD). Composition of FeO was analysed by the wet chemical method. Whole rock trace elements were analysed in GPRM by ICP-MS (Agilent 7500a) after acid digestion ($\text{HF} + \text{HNO}_3$) in high-pressure Teflon bombs. Trace element abundances were determined by a Finnigan Element II ICP-MS, with analytical uncertainties within 5% for most elements. The analytical results are listed in Supplementary Table 2.

4. Results

4.1. Zircon U–Pb dating

Zircon grains from Guiyantou granite sample ZM054-1 are ~160–800 μm long, and prismatic with aspect ratios

of 1:1 to 4:1 (Figure 5). Analyses yield Th/U ratios of 0.64–1.15. Uranium–lead isotope analyses were conducted on 19 zircon grains (Supplementary Table 1; Figure 5(a)). All 19 grains had similar $^{206}\text{Pb}/^{238}\text{U}$ ages, ranging from 212 ± 4 to 247 ± 3 Ma. Twelve analyses cluster on the concordia diagram and yield a weighted mean $^{206}\text{Pb}/^{238}\text{U}$ age of 232 ± 4 Ma (MSWD = 1.12), which is interpreted to represent the igneous crystallization age.

Zircon grains from Guiyantou granite sample ZM055-1 are prismatic and automorphic, and mostly 150–200 μm long. They show incomplete oscillatory magmatic zoning, and yield Th/U ratios of 0.23–1.31. Uranium–lead isotope analyses were conducted on 15 zircon grains (Supplementary Table 1; Figure 5(b)). One analysis yielded a $^{206}\text{Pb}/^{238}\text{U}$ age of 130 Ma. The remaining 14 zircon grains yielded $^{206}\text{Pb}/^{238}\text{U}$ ages of 193 ± 2 Ma to 259 ± 3 Ma, from which four grains yielded concordant U–Pb ages with a weighted mean $^{206}\text{Pb}/^{238}\text{U}$ age of 231 ± 7 Ma (MSWD = 2.0), which is interpreted as the igneous crystallization age of the granite. The zircon measurements that did not fall on the concordia curve might have experienced a loss of radioactive ^{206}Pb .

Zircon grains from the Luoguyan granite sample ZM059-1 are elongate and prismatic, and ~ 80 – 300 μm

long. Analyses yield Th/U ratios of 0.48–0.86. The CL images show strong oscillatory zoning (Figure 5(c)). Uranium–lead isotope analyses were conducted on 20 zircon grains (Supplementary Table 1; Figure 5(c)). Seventeen analyses cluster on a concordia and yield a weighted mean $^{206}\text{Pb}/^{238}\text{U}$ age of 221 ± 5 Ma (MSWD = 5.5), which is interpreted as the igneous crystallization age.

4.2. Major and trace element contents

The major element concentrations of the Guiyantou and Luoguyan granites are listed in Supplementary Table 2. The two granites have SiO_2 contents of 73.62–78.50 wt.%, high Al_2O_3 contents (12.00–13.46 wt.%), and high alkalis ($\text{Na}_2\text{O}+\text{K}_2\text{O} = 7.14$ – 8.72 wt.%). Both the granites plot in the calc-alkaline granite field on the $(\text{Na}_2\text{O}+\text{K}_2\text{O})$ vs. SiO_2 discrimination diagram (Figure 6(a)), and within the high-K series field on the K_2O vs. SiO_2 discrimination diagram (Figure 6(b)). All the samples have A/CNK (A/CNK = molar ratio of $\text{Al}_2\text{O}_3/(\text{CaO}+\text{K}_2\text{O}+\text{Na}_2\text{O})$) ratios of 0.98–1.05. The samples lie in the metaluminous to weakly peraluminous fields on a plot of A/NK (A/NK = molar ratio of $\text{Al}_2\text{O}_3/(\text{K}_2\text{O}+\text{Na}_2\text{O})$) versus A/CNK (Figure 6(c)).

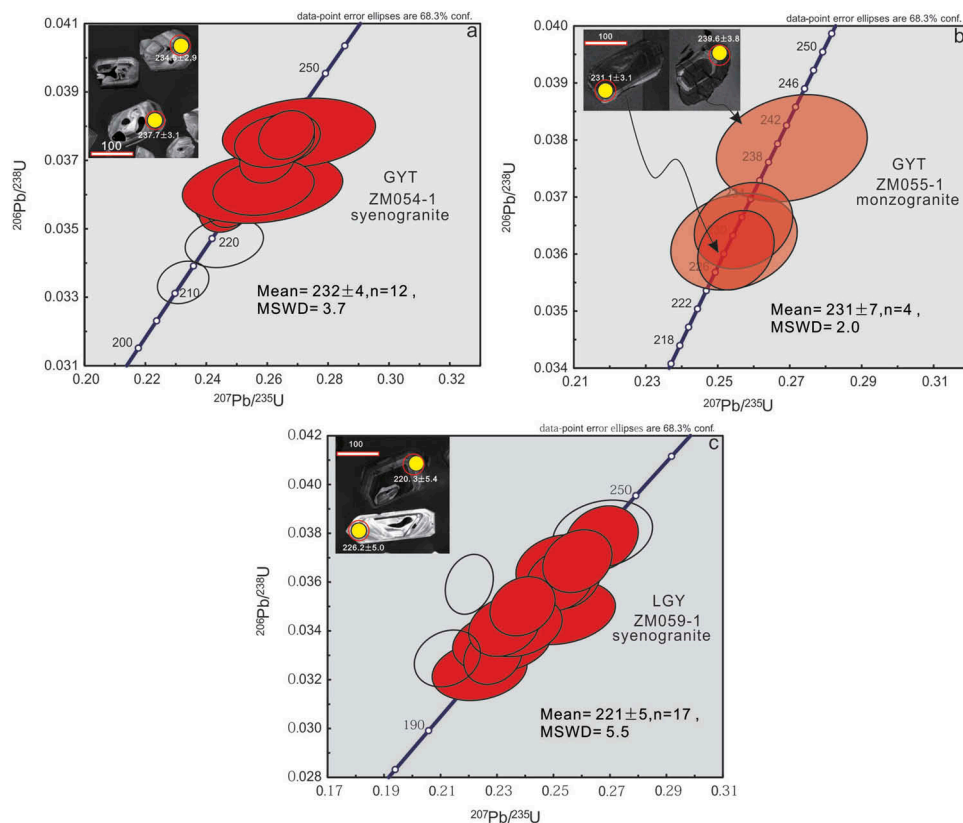


Figure 5. Representative zircon CL images and U–Pb concordia diagrams for the Guiyantou(a and b) and Luoguyan granites (c) showing analytical spots for U–Pb dating (yellow circles) and Hf isotopes (red circles).

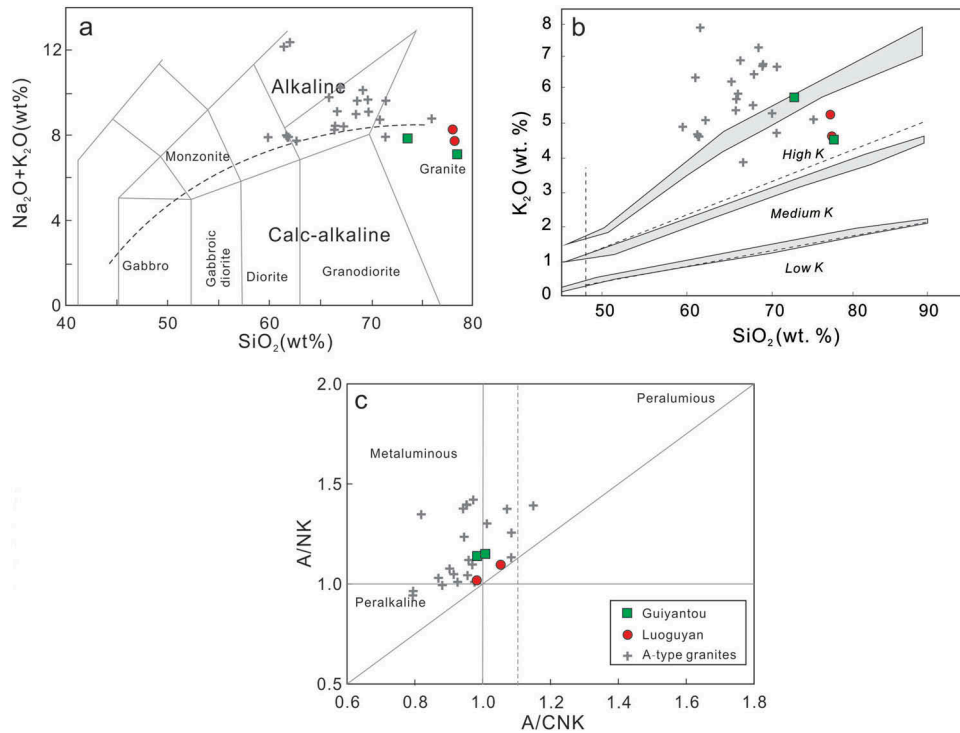


Figure 6. (a) Plot of $\text{Na}_2\text{O} + \text{K}_2\text{O}$ vs. SiO_2 for the Guiyantou and Luoguyan granites (Middlemost, 1994). (b) Plot of K_2O vs. SiO_2 (Le Maitre *et al.*, 1989). (c) Plot of A/NK vs. A/CNK (Maniar and Piccoli, 1989). The data for Triassic A-type granites of SE China are from previous studies (Wang *et al.* 2005b; Sun *et al.* 2011; Li *et al.* 2012a; Mao *et al.* 2013; Zhao *et al.* 2013; Gao *et al.* 2014). A/CNK : molar ratios of $\text{Al}_2\text{O}_3/(\text{CaO} + \text{Na}_2\text{O} + \text{K}_2\text{O})$; A/NK : molar ratios of $\text{Al}_2\text{O}_3/(\text{Na}_2\text{O} + \text{K}_2\text{O})$.

The Guiyantou and Luoguyan granites have total rare earth element (ΣREE) contents of 66–305 ppm. Both the granites are enriched in light rare earth elements (LREE), with LREE/high field-strength element (HREE) ratios of 2–15 and $(\text{La}/\text{Yb})_N$ values of 2–21. On chondrite-normalized diagrams (Figure 7(a)), the LREE display greater enrichment than HREE. The samples show significant negative Eu anomalies ($\delta\text{Eu} = 0.02\text{--}0.31$) consistent with fractional crystallization of plagioclase.

On N-MORB-normalized diagrams (Figure 7(b)), the Guiyantou and Luoguyan granites are enriched in Rb, Th, and K, and depleted in Nb, Ta, Ti, and P. Variations in Rb, Ba, Sr, and Ti contents mainly reflect the proportions of different rock-forming minerals, whereas the low Nb and Ta contents indicate an affinity with continental crust (Barth *et al.* 2000).

4.3. Zircon Hf isotopic compositions

Thirty-four spots on 34 zircon grains from the Guiyantou granite (samples ZM054-1 and ZM055-1) were analysed for Lu–Hf isotopic compositions. The $\epsilon\text{Hf}(t)$ values were calculated at the respective U–Pb age for each zircon and the results are listed in Supplementary Table 3. The $\epsilon\text{Hf}(t)$ values range from –

9.0 to –1.1 (Figure 8(a)) and the corresponding two-stage Hf isotopic model ages vary from 1.84 to 1.33 Ga (Figure 8(b)).

Sixteen spots on 16 zircon grains from the Luoguyan granite (sample ZM059-1) were analysed for Lu–Hf isotopic compositions (Supplementary Table 3), and again the $\epsilon\text{Hf}(t)$ values were calculated at the appropriate U–Pb age for each grain. The $\epsilon\text{Hf}(t)$ values range from –11.5 to –6.0 (Figure 8(c)). The corresponding two-stage Hf isotopic model ages vary from 1.98 to 1.64 Ga (Figure 8(d)).

5. Discussion

5.1. Rock type

The Guiyantou and Luoguyan granites are mostly metaluminous to weakly peraluminous ($\text{A}/\text{CNK} = 0.98\text{--}1.05$), and contain high concentrations of SiO_2 (73.62–78.50 wt. %), and low concentrations of MgO (0.12–0.32 wt. %), all of which are indicative of partial melting of crustal material. The high- SiO_2 granites within the pluton contain intermediate to high concentrations of K_2O that are similar to melts produced by the partial melting of intermediate to mafic rocks (Sisson *et al.* 2005). Most of samples plot near to the boundary between A-type, I-type, and

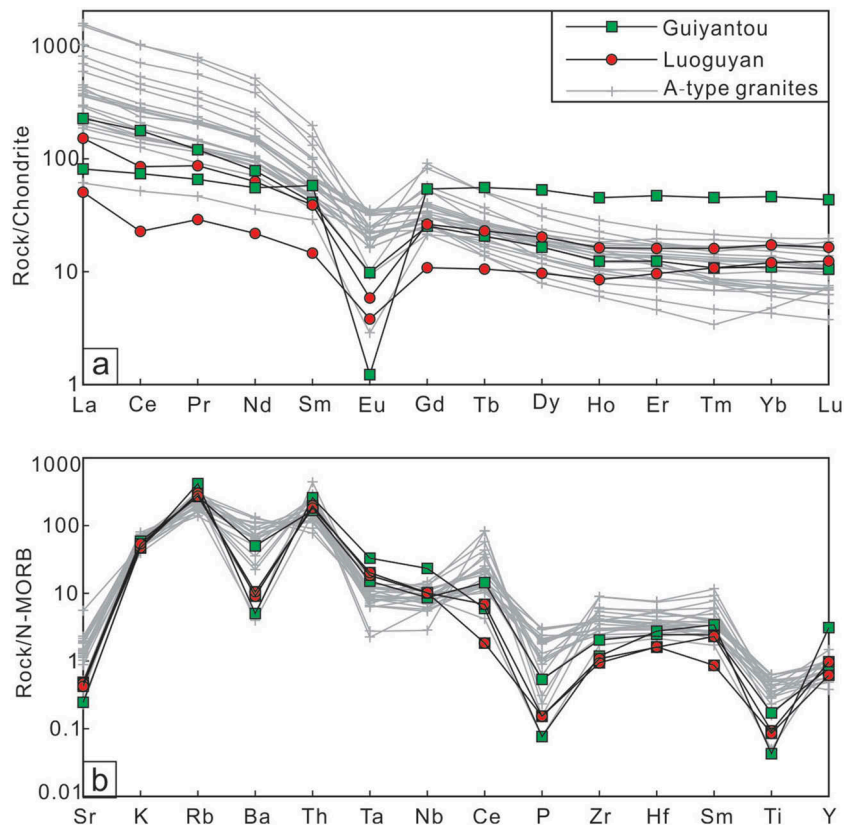


Figure 7. (a) Chondrite-normalized REE patterns (Boynnton, 1984) and (b) N-MORB-normalized spider diagram (Sun and McDonough, 1989) for the Guiyantou and Luoguyan granites. The data for the A-type granites are the same as those used for Figure 6.

S-type granites (Figure 9(a,b); Whalen *et al.* 1987), and plot in the field of ferroan granites (Figure 9(c); Frost *et al.* 2001). All the samples formed at a temperature as those of typical A-type granites (800–900°C) as shown in Figure 9(d). Even though the Zr + Nb + Ce + Y contents are lower than those of A-type granites (≥ 350 ppm; (Whalen *et al.* 1987), except for sample ZM054-2 (Supplementary Table 2). This suggests that the Guiyantou and Luoguyan granites are metaluminous to weakly peraluminous high-K A-type granites derived from partial melting of metamorphic rocks within the lower crust just as Dengfuxian A-type granite in Hunan (Cai *et al.* 2015).

5.2. Source and petrogenesis

The origins of Triassic A-type granites in eastern SCB are still the subject of debate (Zhao *et al.* 2013; Zhu *et al.* 2016). The focus of the debate is whether the mantle material participation in the generation of A-type or not. The Guiyantou and Luoguyan granites have geochemical characteristics of A-type granites, with high Al_2O_3 (12.88–15.10 wt.%), alkalis ($\text{K}_2\text{O} + \text{Na}_2\text{O} = 7.96\text{--}8.44$ wt.%), $\text{K}_2\text{O}/\text{Na}_2\text{O}$ (1.9–7.97), and

ACNK (0.98–1.05). The Rb/Ba and Rb/Sr values of the A-type granites (including Guiyantou and Luoguyan granites) are shown in Figure 10 and demonstrate that these granites were possibly derived from a meta-sedimentary source. Also in the K_2O vs SiO_2 diagram (Figure 6(b)), most of A-type granites plotted in the high-K region. High-K granitic magmas are considered to form under two types of collisional setting: melting of crustal rocks by crustal thickening or decompression and contamination of parent mantle melts by crustal material during their ascent (Song *et al.* 2017). It is unlikely that the granitoids were generated directly from the mantle because there are no coeval large-scale mafic igneous intrusions or abundant mafic enclaves, and the SiO_2 contents of our samples are very high (>70 wt.%).

Zircon, as an early crystallizing mineral from granitic magma, commonly retains its original isotopic composition, and thus it is widely used to trace petrogenetic processes (Griffin *et al.* 2002). Zircon from the Guiyantou granite has $\epsilon\text{Hf}(t)$ values ranging from –9 to –1.1 with corresponding T_{DM}^{C} ages of 1.84–1.33 Ga (Figure 8). Zircon from the Luoguyan granite has $\epsilon\text{Hf}(t)$ values ranging from –6.0 to –11.5 with corresponding

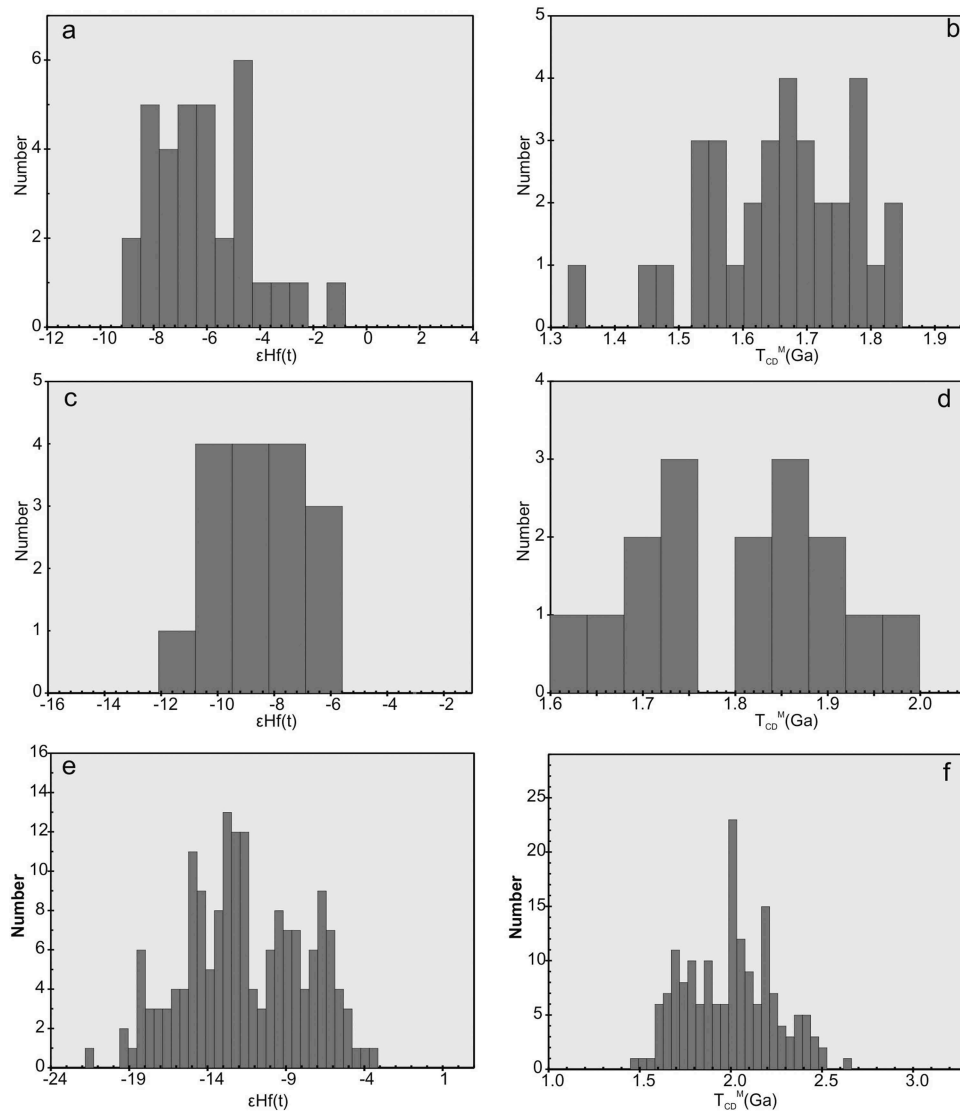


Figure 8. Zircon Hf isotopic compositions of the Guiyantou and Luoguyan granites. (a–b) Histograms of the zircon $\epsilon\text{Hf}(t)$ values and the TDMC (Ga) for the Guiyantou granite. (c–d) Histograms of the zircon $\epsilon\text{Hf}(t)$ values and TDMC (Ga) of the Luoguyan granite. (e–f) Histograms of the zircon $\epsilon\text{Hf}(t)$ values and TDMC (Ga) of the A-type granites. The data for Triassic A-type granites of SE China are from previous studies (Sun *et al.* 2011; Li *et al.* 2012a; Wang *et al.*, 2013b; Zhao *et al.* 2013; Gao *et al.* 2014).

T_{DM}^{C} ages from 1.64 to 1.98 Ga (Figure 8). In $\epsilon\text{Hf}(t)$ vs. age diagram (Figure 11), most Hf isotopic data of Triassic A-type granites are plotted under the Chur line, suggesting crustal source.

An extensive survey of the Nd isotope compositions of Phanerozoic igneous rocks across the Cathaysia block led to the conclusion that the crust of southeast China formed in the Proterozoic (Xu *et al.* 2007). For the Guiyantou and Luoguyan granites, two-stage zircon Hf model ages of 1.3–2.0 Ga indicate that Paleoproterozoic rocks might be the source of the Triassic granites. The Mayuan Group in northwestern Fujian Province has been regarded as Paleoproterozoic basement (Yu *et al.* 2012), and also appears to be an appropriate source candidate. However, many Precambrian basement rocks

in the Cathaysia block previously considered as Paleoproterozoic to Mesoproterozoic are actually Neoproterozoic (Zhao 2015). If Neoproterozoic rocks with Paleoproterozoic model ages were partially melted in the Triassic, the magmas generated will inherit Paleoproterozoic model ages. In this case, the source rocks of the Triassic granites would be Neoproterozoic rather than Paleoproterozoic. In addition, more and more studies have shown that there are abundant Neoproterozoic inherited zircon grains within Triassic granites from all over south China (Fu *et al.* 2015; Qiao *et al.* 2015; Gao *et al.* 2016, 2017). Those inherited zircons could provide direct age information about the source rocks. From the studies on the zircon data in previous studies, we infer that the Guiyantou and

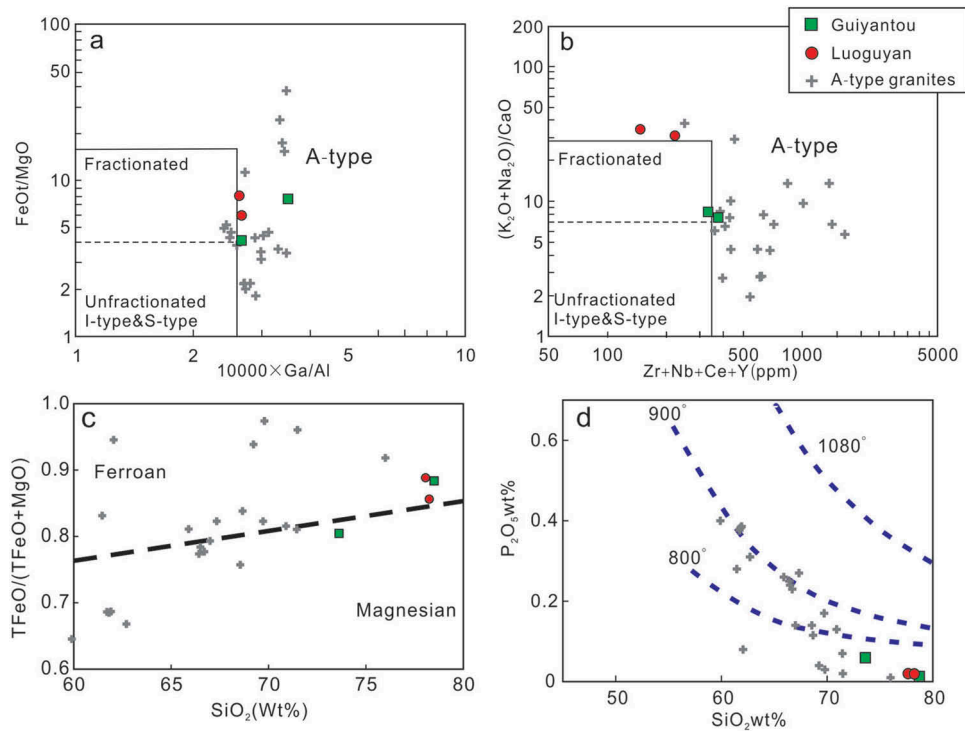


Figure 9. Samples of the Guiyantou and Luoguyan granites on plots of (a) FeOT/MgO vs. $10000 \times \text{Ga}/\text{Al}$ (Whalen *et al.* 1987), (b) $(\text{K}_2\text{O}+\text{Na}_2\text{O})/\text{CaO}$ vs. $\text{Zr} + \text{Nb} + \text{Ce} + \text{Y}$ (Whalen *et al.* 1987), (c) $\text{FeOT}/(\text{FeOT} + \text{MgO})$ vs. SiO_2 (Frost *et al.* 2001), and (d) P_2O_5 vs. SiO_2 (Harrison and Watson, 1984). The data for the A-type granites are the same as those used for Figure 6.

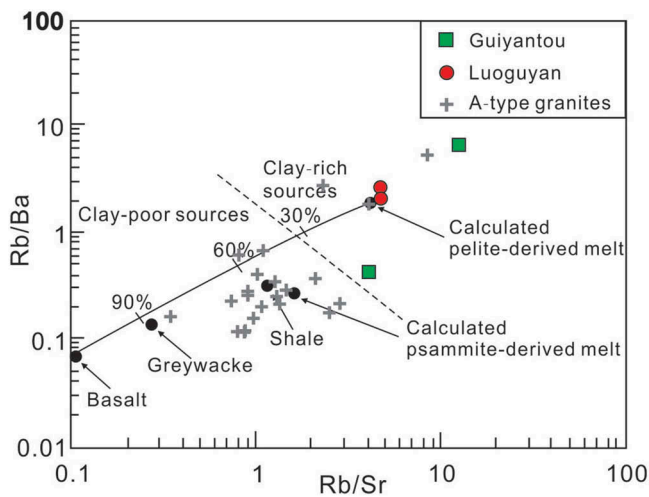


Figure 10. Plot of Rb/Ba vs. Rb/Sr (Sylvester, 1989) for the Guiyantou and Luoguyan granites. The data for the A-type granites are the same as those used for Figure 6.

Luoguyan granites were derived from partial melting of Neoproterozoic basement rocks of the Cathaysia block.

5.3. Tectonic implications

The widely distributed Triassic magmatic rocks in southeast China have long been studied in order to define

the early Mesozoic tectonic history of the SCB and East Asia (Zhou *et al.* 2006; Li and Li 2007). Some studies pointed out that calc-alkaline plutons in Hainan island might be interpreted as evidence for oceanic subduction of the paleo-Pacific plate recorded in the eastern part of the southeast Asian continental margin and southeastern coastal areas of south China (Li *et al.* 2006, 2012b, 2012c). The presence of Triassic A-type granitoids in SCB is consistent with an Early Mesozoic Andean-type (Cordillera-type) orogeny (Zhu *et al.* 2014, 2016). Wang *et al.* (2013b) proposed that the A-type granite was emplaced in a continental back-arc related to the early Mesozoic Pacific Plate subduction had affected Fujian and Zhejiang provinces. In addition, one hypothesis has proposed the NE-trending distribution A-type granite belt might be controlled by NE-trending strike-slip faults in response to the subduction of the paleo-Pacific Plate underneath the SCB (Sun *et al.* 2011). However, the distribution of the Triassic granites does not display any temporal-spatial propagation of age trend from the coast towards the cratonic interior of South China and arc-related magmatic rock assemblages were absent in South China so far (Wang *et al.* 2013a; Shu *et al.* 2015; Song *et al.* 2015). Recent studies emphasized an intracontinental tectonic event as the major mechanism for the early Mesozoic tectonic event (Chu *et al.* 2012b, 2012c; Song *et al.* 2015, 2016, 2017;

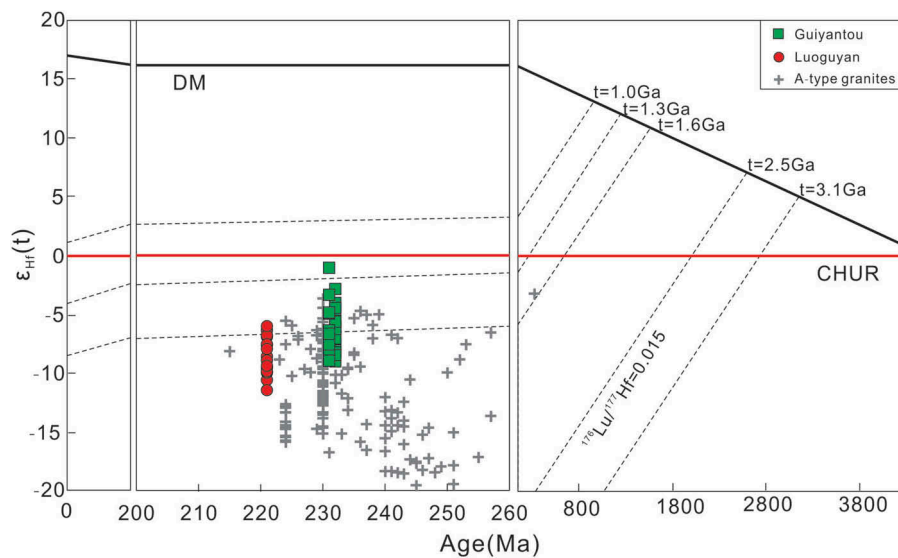


Figure 11. Hafnium isotopic compositions of zircon from the Guiyantou and Luoguyan granites. Compositions of zircon from Triassic A-type granites in SE China are from previous studies (Zhao *et al.* 2013; Wang *et al.* 2013b; Gao *et al.* 2014, 2017).

Faure *et al.* 2016, 2017). During the Late Permian to Early Triassic, closure of the Paleo-Tethys Ocean and subsequent collision of the Indochina Block with the SCB in the south, and intracontinental subduction between the SCB and North China Block occurred along the Qinling–Dabie–Sulu orogenic belt (Faure *et al.* 2008; Wu and Zheng 2013) in the north together drove intracontinental orogenesis across the SCB (Zhang *et al.* 2013; Wang *et al.* 2013a; Shu *et al.* 2015). During the formation of orogens surrounding the SCB, tectonic stress generated along the craton boundaries might have propagated into the cratonic interior (Song *et al.* 2017). With the propagating of this process, the thickening and shortening of the crust provided additional heat to meet the requirements of the crustal partial melting in the Early Triassic. Uranium–lead zircon ages for metamorphism reported for Wuyi–Yunkai and Nanling tectonic belt are mostly concentrated between 253 and 233 Ma (Xiang *et al.* 2008; Wang *et al.* 2012; Zhao *et al.* 2012), indicating a compressional environment during the Early Triassic, consistent with strong folding, thrust faulting, and nappes developed at this time (Lin *et al.* 2001, 2008; Wang *et al.* 2005c, 2007b; Zhang *et al.* 2009; Chu *et al.* 2012b; Faure *et al.* 2016). With stress relaxation and intracontinental extension, the Late Triassic granitic magma in the SCB was generated and emplaced under post-collisional setting.

Our new zircon LA–ICP–MS U–Pb age data for the Guiyantou and Luoguyan granites yield Late Triassic emplacement ages of, respectively, 232 and 221 Ma. The Guiyantou and Luoguyan granites also define a high-K A-type suite, which plots in the post-collisional granite field on a Rb vs. Y+Nb diagram (Figure 12).

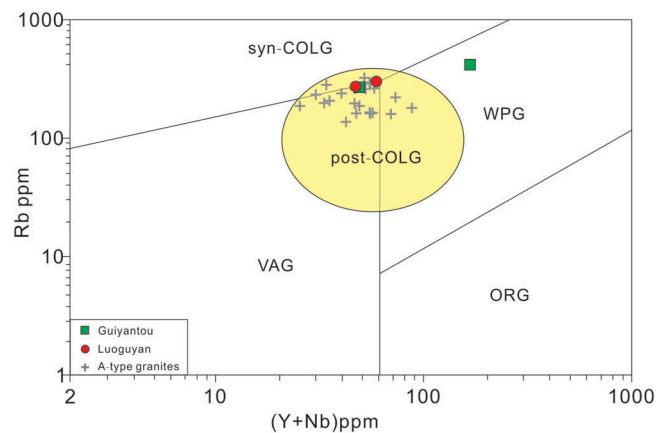


Figure 12. Samples of the Guiyantou and Luoguyan granites plotted on a discrimination diagram of Rb vs. (Y+Nb) (Pearce, 1996). Symbols as in Figure 6. WPG = within-plate granite, VAG = volcanic arc granite, syn-COLG = syn-collisional granite, ORG = 628 oceanic ridge granite. The data for the A-type granites are the same as those used for Figure 6.

Contemporaneous intrusions have also been reported along the coastal region of the SCB and include the Wengshan A-type granites (232 Ma) (Sun *et al.* 2011), Jingju and Dashuang A-type granites (246–215 Ma) (Li *et al.* 2012a; Mao *et al.* 2013; Gao *et al.* 2014; Zhu *et al.* 2016), Gaoxi and Caijiang A-type granites (230–228 Ma) (Zhao *et al.* 2013), Dayinchang A-type granite (237–228 Ma) (Wang *et al.* 2013b), Guikeng granite (234–220 Ma) (Mao *et al.* 2011), and Xiaotao granite (222 Ma) (Wang *et al.* 2007c). All these A-type granites are commonly considered to be restricted to anorogenic environments, they also occur in the post-collisional tectonic setting (Milani *et al.* 2015). The U–Pb

ages for Triassic A-type granites in the coastal region of the SCB mainly vary from 232 to 215 Ma, with most emplaced between 230 and 225 Ma. Emplacement of the Guiyantou and Luoguyan granites, with the 230–225 Ma A-type granites may mark the beginning of extension after the collisions around the SCB (Cai *et al.* 2015). Intrusion of the Xiamao diabase, with an age of 223 ± 2 Ma in the east of Wuyi Mountain, and gabbro xenoliths with ages of 224 Ma in the Daoxian region (Guo *et al.* 1997) indicates that extension and thinning was from the beginning of the late Triassic that followed the Early to Middle Triassic collision (Wang *et al.* 2013b). Thus, heat from underplating of mantle-derived material may play a role in the melt of

the granitic magma (Song *et al.* 2017). Furthermore, the thickening and shortening process of the continental interior might have produced substantial heat to increase the temperature of the mid- to lower crust. Triassic A-type granites in the coastal region of the SCB and many other Triassic magnesian (I- and S-type) granitoids in the central-western SCB, which displayed planar-shaped distribution and were mainly derived from a pelitic-derived source with no evidence for significant involvement of mantle-derived components dated at 200–240 Ma (Wang *et al.* 2013a; Shu *et al.* 2015). Magma derived from high-temperature partial melting of residual granulite formed a series of planar-shaped peraluminous granitic intrusions in

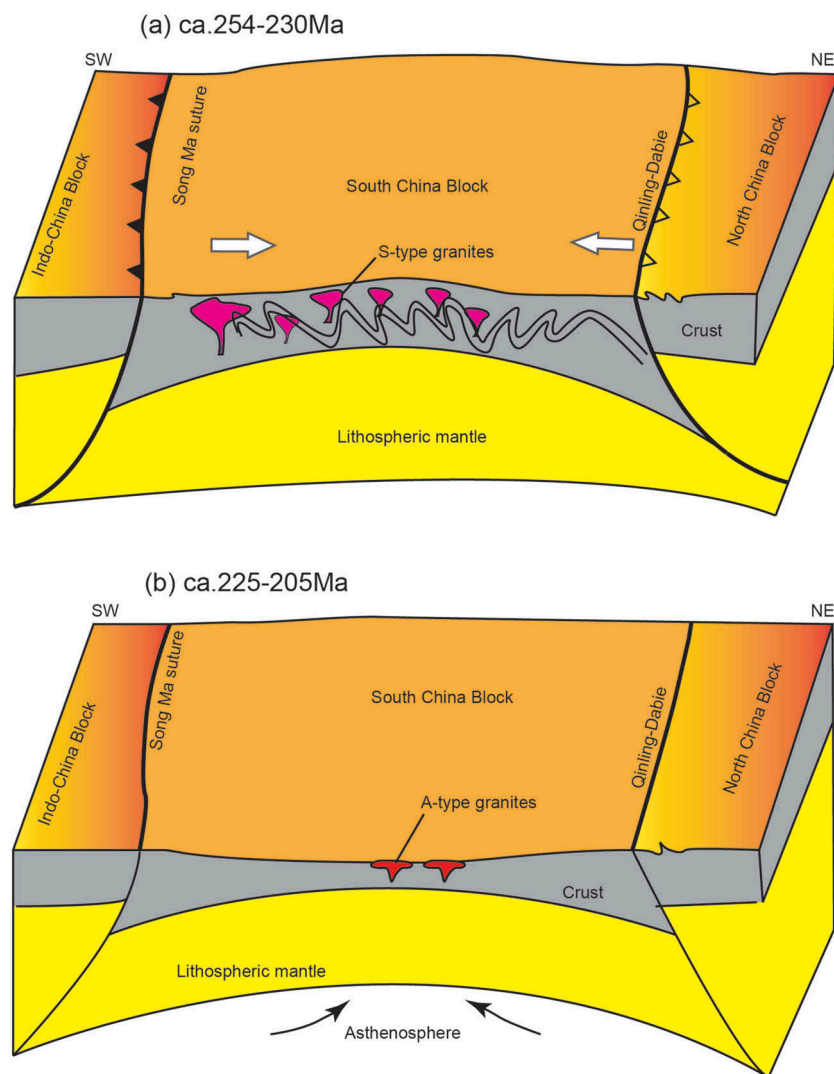


Figure 13. Cartoon showing the driving mechanisms for the Triassic granites in the South China Block; (a) during c. 254–230 Ma, the collision between the Indo-China Block and the South China Craton, and intracontinental collision between SCB and North China Craton, caused intracontinental orogeny in South China, resulting in the thickening and shortening of the crust and the generation of abundant syn-orogenic peraluminous granites in South China; (b) during c. 225–205 Ma, with stress relaxation and intracontinental extension, the Late Triassic granitic magma in the SCB was generated and emplaced under post-collisional setting, and the crust caused partial melting of the lower crust formed a series of Late Triassic A-type granites in the coastal region of the SCB.

the SE-SCB (Figure 13). Under an extensional tectonic regime, crustal denudation and thinning finally contributed to the ascent and emplacement of the magma.

6. Conclusions

Our LA-ICP-MS U-Pb zircon dating shows that the Guiyantou and Luoguyan granites intruded Precambrian basement in the Middle-Late Triassic at 232 ± 2 and 221 ± 3 Ma, respectively. *In situ* Hf isotopic analyses of zircon indicate that these granites formed by partial melting of Neoproterozoic rocks of the Cathaysia block. The Triassic A-type granites along the southeastern margin of the SCB probably formed during the post-orogenic extensional that followed the Early to Middle Triassic collision between the SCB and a southern unexposed block.

Acknowledgements

The authors are grateful to Prof. Michel Faure, Prof. Xinqi Yu and an anonymous reviewer for their extremely useful comments, especially Prof. Michel Faure, who significantly improved the manuscript. We are indebted to Tao Qian, Li Gao, Mingming Cui, and Yongyan Guo for assistance with the zircon LA-ICP-MS analyses.

Disclosure statement

No potential conflict of interest was reported by the authors.

Funding

This study was supported by National Natural Science Foundation of China [No. 41702204], the Central Fundamental Research (grant number DZLXJK201504), and the Major State Research Development Program of China (grant number 2016YFC0600202).

References

- Andersen, T., 2002, Correction of common lead in U-Pb analyses that do not report 204Pb: *Chemical Geology*, v. 192, p. 59–79. doi:10.1016/S0009-2541(02)00195-X
- Barth, M.G., McDonough, W.F., and Rudnick, R.L., 2000, Tracking the budget of Nb and Ta in the continental crust: *Chemical Geology*, v. 165, p. 197–213. doi:10.1016/S0009-2541(99)00173-4
- Blichert-Toft, J., and Albarède, F., 1997, The Lu-Hf isotope geochemistry of chondrites and the evolution of the mantle-crust system: *Earth and Planetary Science Letters*, v. 148, p. 243–258. doi:10.1016/S0012-821X(97)00040-X
- Boynton, W.L. 1984, Geochemistry of the rare earth elements: Meteorite studies, in Henderson, P., ed., *Rare earth element geochemistry*: Amsterdam, Elsevier, p. 63–114.

- Cai, Y., Lu, J.J., Ma, D.S., Huang, H., Zhang, H.F., and Zhang, R. Q., 2015, The Late Triassic Dengfuxian A-type granite, Hunan Province: Age, petrogenesis, and implications for understanding the late Indosinian tectonic transition in South China: *International Geology Review*, v. 57, p. 428–445. doi:10.1080/00206814.2015.1012565
- Charvet, J., Shu, L., Faure, M., Choulet, F., Wang, B., Lu, H., and Breton, N.L., 2010, Structural development of the Lower Paleozoic belt of South China: Genesis of an intracontinental orogen: *Journal of Asian Earth Sciences*, v. 39, p. 309–330. doi:10.1016/j.jseas.2010.03.006
- Chu, N.C., Taylor, R.N., Chavagnac, V., Nesbitt, R.W., Boella, R.M., Milton, J.A., German, C.R., Bayon, G., and Burton, K., 2002, Hf isotope ratio analysis using multi-collector inductively coupled plasma mass spectrometry: An evaluation of isobaric interference corrections: *Journal of Analytical Atomic Spectrometry*, v. 17, p. 1567–1574. doi:10.1039/b206707b
- Chu, Y., Faure, M., Lin, W., and Wang, Q., 2012b, Early Mesozoic tectonics of the South China block: Insights from the Xuefengshan intracontinental orogen: *Journal of Asian Earth Sciences*, v. 61, p. 199–220. doi:10.1016/j.jseas.2012.09.029
- Chu, Y., Faure, M., Lin, W., Wang, Q., and Ji, W., 2012c, Tectonics of the Middle Triassic intracontinental Xuefengshan Belt, South China: New insights from structural and chronological constraints on the basal décollement zone: *International Journal of Earth Sciences*, v. 101, p. 2125–2150. doi:10.1007/s00531-012-0780-5
- Chu, Y., Lin, W., Faure, M., Wang, Q., and Ji, W., 2012a, Phanerozoic tectonothermal events of the Xuefengshan Belt, central South China: Implications from UPb age and LuHf determinations of granites: *Lithos*, v. 150, p. 243–255. doi:10.1016/j.lithos.2012.04.005
- Dall'Agnol, R., Frost, C.D., and Rämö, O.T., 2012, IGCP Project 510 “A-type Granites and Related Rocks through Time”: Project vita, results, and contribution to granite research: *Lithos*, v. 151, p. 1–16. doi:10.1016/j.lithos.2012.08.003
- Eby, G.N., 1990, The A-type granitoids: A review of their occurrence and chemical characteristics and speculations on their petrogenesis: *Lithos*, v. 26, p. 115–134. doi:10.1016/0024-4937(90)90043-Z
- Faure, M., Chen, Y., Feng, Z., Shu, L., and Xu, Z., 2017, Tectonics and geodynamics of South China: An introductory note: *Journal of Asian Earth Sciences*, v. 141, p. 1–6. doi:10.1016/j.jseas.2016.11.031
- Faure, M., Lin, W., Chu, Y., and Lepvrier, C., 2016, Triassic tectonics of the southern margin of the South China Block: *Comptes Rendus Geoscience*, v. 348, p. 5–14. doi:10.1016/j.crte.2015.06.012
- Faure, M., Lin, W., Monié, P., and Meffred, S., 2008, Palaeozoic collision between the North and South China Blocks, Triassic intracontinental tectonics, and the problem of the ultrahigh-pressure metamorphism: *Comptes Rendus Geoscience*, v. 340, p. 139–150. doi:10.1016/j.crte.2007.10.007
- Faure, M., Shu, L., Wang, B., Charvet, J., Choulet, F., and Monie, P., 2009, Intracontinental subduction: A possible mechanism for the Early Palaeozoic Orogen of SE China: *Terra Nova*, v. 21, p. 360–368. doi:10.1111/ter.2009.21.issue-5
- Förster, H.J., Tischendorf, G., and Trumbull, R.B., 1997, An evaluation of the Rb vs. (Y + Nb) discrimination diagram to infer tectonic setting of silicic igneous rocks: *Lithos*, v. 40, p. 261–293. doi:10.1016/S0024-4937(97)00032-7

- Frost, B.R., Barnes, C.G., Collins, W.J., Arculus, R.J., Ellis, D.J., and Frost, C.D., 2001, A geochemical classification for granitic rocks: *Journal of Petrology*, v. 42, p. 2033–2048. doi:10.1093/petrology/42.11.2033
- Fu, S.L., Hu, R.Z., Bi, X.W., Chen, Y.W., Yang, J.H., and Huang, Y., 2015, Origin of Triassic granites in central Hunan Province, South China: Constraints from zircon U-Pb ages and Hf and O isotopes: *International Geology Review*, v. 57, p. 97–111. doi:10.1080/00206814.2014.996258
- Gao, P., Zheng, Y., and Zhao, Z., 2016, Distinction between S-type and peraluminous I-type granites: Zircon versus whole-rock geochemistry: *Lithos*, v. 258–259, p. 77–91. doi:10.1016/j.lithos.2016.04.019
- Gao, P., Zheng, Y., and Zhao, Z., 2017, Triassic granites in South China: A geochemical perspective on their characteristics, petrogenesis, and tectonic significance: *Earth-Science Reviews*, v. 173, p. 266–294. doi:10.1016/j.earsci.2017.07.016
- Gao, W.L., Wang, Z.X., Song, W.J., Wang, D.X., and Li, C.L., 2014, Zircon U–Pb geochronology, geochemistry and tectonic implications of Triassic A-type granites from southeastern Zhejiang, South China: *Journal of Asian Earth Sciences*, v. 96, p. 255–268. doi:10.1016/j.jseas.2014.09.024
- Griffin, W.L., Wang, X., Jackson, S.E., Pearson, N.J., O'Reilly, S.Y., Xu, X., and Zhou, X., 2002, Zircon chemistry and magma mixing, SE China: In-situ analysis of Hf isotopes, Tonglu and Pingtan igneous complexes: *Lithos*, v. 61, p. 237–269. doi:10.1016/S0024-4937(02)00082-8
- Guo, F., Fan, W., Lin, G., and Lin, Y., 1997, Sm–Nd isotopic age and genesis of gabbro xenoliths in Daoxian County, Hunan Province: *Chinese Science Bulletin*, v. 42, p. 1814–1817. doi:10.1007/BF02882650
- Guo, J., Wu, Y., Gao, S., Jin, Z., Zong, K., Hu, Z., Chen, K., Chen, H., and Liu, Y., 2015, Episodic Paleoproterozoic (3.3–2.0 Ga) granitoid magmatism in Yangtze Craton, South China: Implications for late Archean tectonics: *Precambrian Research*, v. 270, p. 246–266. doi:10.1016/j.precamres.2015.09.007
- Harrison, T.M., and Watson, E.B., 1984, The behavior of apatite during crustal anatexis: Equilibrium and kinetic considerations: *Geochimica et Cosmochimica Acta*, v. 48, no. 7, p. 1467–1477.
- Hou, K.J., Li, Y.H., and Tian, Y.R., 2009, In situ U–Pb zircon dating using laser ablation multi-collector counting- ICP-MS: *Mineral Deposits*, v. 28, p. 481–492. (in Chinese with English abstract).
- Hou, K.J., Li, Y.H., Zhou, T.R., Qu, X.M., Shi, Y.R., and Xie, G.Q., 2007, Laser ablation-MCICP-MS technique for Hf isotope microanalysis of zircon and its geological applications: *Acta Petrol Sinica*, v. 23, p. 2595–2604. (in Chinese with English abstract).
- Le Maitre, R.W., Bateman, P., Dudek, A., Keller, J., Lameyre, J., Lebas, M.J., Sabine, P.A., Schmin, R., Sorensen, H., Streckeisen, A., Wooley, A.R., and Zanettin, B., 1989, A classification of igneous rocks and glossary of terms: Oxford, Blackwell.
- Li, J.H., Zhang, Y.Q., Dong, S.W., Su, J.B., Li, Y., Cui, J.J., and Shi, W., 2013, The Hengshan low-angle normal fault zone: Structural and geochronological constraints on the Late Mesozoic crustal extension in South China: *Tectonophysics*, v. 606, p. 97–115. doi:10.1016/j.tecto.2013.05.013
- Li, W., Li, X., Li, Z., and Lou, F., 2008, Obduction-type granites within the NE Jiangxi Ophiolite: Implications for the final amalgamation between the Yangtze and Cathaysia Blocks: *Gondwana Research*, v. 13, p. 288–301. doi:10.1016/j.gr.2007.12.010
- Li, W.Y., Ma, C.Q., Liu, Y.Y., and Robinson, P.T., 2012a, Discovery of the Indosinian aluminum A-type granite in Zhejiang Province and its geological significance: *Science in China Series D: Earth Science*, v. 55, p. 13–25. doi:10.1007/s11430-011-4351-6
- Li, X.H., 2000, Cretaceous magmatism and lithospheric extension in Southeast China: *Journal of Asian Earth Sciences*, v. 18, p. 293–305. doi:10.1016/S1367-9120(99)00060-7
- Li, X.H., Li, Z.X., He, B., Li, W.X., Li, Q.L., Gao, Y.Y., and Wang, X.C., 2012b, The Early Permian active continental margin and crustal growth of the Cathaysia Block: In situ U–Pb, Lu–Hf and O isotope analyses of detrital zircons: *Chemical Geology*, v. 328, p. 195–207. doi:10.1016/j.chemgeo.2011.10.027
- Li, X.H., Li, Z.X., Li, W.X., and Wang, Y.J., 2006, Initiation of Indosinian Orogeny in South China—Evidence for a Permian Magmatic Arc on Hainan Island: *The Journal of Geology*, v. 114, p. 341–353. doi:10.1086/501222
- Li, Z.X., and Li, X.H., 2007, Formation of the 1300-km-wide intracontinental orogen and postorogenic magmatic province in Mesozoic South China: A flat-slab subduction model: *Geology*, v. 35, p. 179–182. doi:10.1130/G23193A.1
- Li, Z.X., Li, X.H., Chung, S.L., Lo, C.H., Xu, X.S., and Li, W.X., 2012c, Magmatic switch-on and switch-off along the South China continental margin since the Permian: Transition from an Andean-type to a Western Pacific-type plate boundary: *Tectonophysics*, v. 532–535, p. 271–290. doi:10.1016/j.tecto.2012.02.011
- Lin, W., Faure, M., Sun, Y., Shu, L., and Wang, Q., 2001, Compression to extension switch during the Middle Triassic orogeny of Eastern China: The case study of the Jiulingshan massif in the southern foreland of the Dabieshan: *Journal of Asian Earth Sciences*, v. 20, p. 31–43. doi:10.1016/S1367-9120(01)00020-7
- Lin, W., Wang, Q., and Chen, K., 2008, Phanerozoic tectonics of south China block: New insights from the polyphase deformation in the Yunkai massif: *Tectonics*, v. 27, p. TC6004. doi:10.1029/2007TC002207
- Liu, Y.S., Hu, Z.C., Gao, S., Gunther, D., Xu, J., Gao, C.G., and Chen, H.H., 2008, In situ analysis of major and trace elements of anhydrous minerals by LA-ICP-MS without applying an internal standard: *Chemical Geology*, v. 257, p. 34–43. doi:10.1016/j.chemgeo.2008.08.004
- Ludwig, K.R., 2001, User's manual for Isoplot/Ex (rev. 2.49): A geochronological toolkit for Microsoft excel: Berkeley Geochronology Centre, Special Publication Vol. 1a, p. 55.
- Maniar, P.D., and Piccoli, P.M., 1989, Tectonic discrimination of granitoids: *Geological Society of America Bulletin*, v. 101, no. 5, p. 635–643.
- Mao, J.R., Takahashi, Y., Kee, W.S., Li, Z.L., Ye, H.M., Zhao, X.L., Liu, K., and Zhou, J., 2011, Characteristics and geodynamic evolution of Indosinian magmatism in South China: A case study of the Guikeng pluton: *Lithos*, v. 127, p. 535–551. doi:10.1016/j.lithos.2011.09.011
- Mao, J.R., Ye, H.M., Liu, K., Li, Z.L., Takahashi, Y., Zhao, X.L., and Kee, W., 2013, The Indosinian collision–Extension event between the South China Block and the Palaeo-Pacific

- plate: Evidence from Indosinian alkaline granitic rocks in Dashuang, eastern Zhejiang, South China: *Lithos*, v. 172–173, p. 81–97. doi:10.1016/j.lithos.2013.04.004
- Middlemost, E.A.K., 1994, Naming materials in the magma/igneous rock system: *Earth-Science Reviews*, v. 37, p. 215–224.
- Milani, L., Lehmann, J., Naydenov, K.V., Saalman, K., Kinnaird, J.A., Daly, J.S., Frei, D., and Lobo-Guerrero Sanz, A., 2015, A-type magmatism in a syn-collisional setting: The case of the Pan-African Hook Batholith in Central Zambia: *Lithos*, v. 216–217, p. 48–72. doi:10.1016/j.lithos.2014.11.029
- Pearce, J.A., 1996, Sources and settings of granitic rocks: *Episode*, v. 19, p. 120–125
- Qiao, L., Wang, Q., and Li, C., 2015, The western segment of the suture between the Yangtze and Cathaysia blocks: Constraints from inherited and co-magmatic zircons from Permian S-type granitoids in Guangxi, South China: *Terra Nova*, v. 27, p. 392–398. doi:10.1111/ter.12171
- Scherer, E., Munker, C., and Merzger, K., 2001, Calibration of the Lutetium Clock: *Science*, v. 293, p. 683–687. doi:10.1126/science.1061372
- Shu, L., Wang, B., Cawood, P.A., Santosh, M., and Xu, Z., 2015, Early Paleozoic and Early Mesozoic intraplate tectonic and magmatic events in the Cathaysia Block, South China: *Tectonics*, v. 34, p. 1–22. doi:10.1002/2015TC003835
- Shu, L.S., Faure, M., Yu, J.H., and Jahn, B.M., 2011, Geochronological and geochemical features of the Cathaysia block (South China): New evidence for the Neoproterozoic breakup of Rodinia: *Precambrian Research*, v. 187, p. 263–276. doi:10.1016/j.precamres.2011.03.003
- Sisson, T.W., Ratajeski, K., Hankins, W.B., and Glazner, A.F., 2005, Voluminous granitic magmas from common basaltic sources: Contributions to Mineralogy & Petrology, v. 148, p. 635–661. doi:10.1007/s00410-004-0632-9
- Song, M., Shu, L., and Santosh, M., 2016, Early Mesozoic granites in the Nanling Belt, South China: Implications for intracontinental tectonics associated with stress regime transformation: *Tectonophysics*, v. 676, p. 148–169. doi:10.1016/j.tecto.2016.03.023
- Song, M., Shu, L., and Santosh, M., 2017, Early Mesozoic intracontinental orogeny and stress transmission in South China: Evidence from Triassic peraluminous granites: *Journal of the Geological Society*, v. 174, p. 591–607. doi:10.1144/jgs2016-098
- Song, M., Shu, L., Santosh, M., and Li, J., 2015, Late Early Paleozoic and Early Mesozoic intracontinental orogeny in the South China Craton: Geochronological and geochemical evidence: *Lithos*, v. 232, p. 360–374. doi:10.1016/j.lithos.2015.06.019
- Streckeisen, A., 1976, To each plutonic rock its proper name: *Earth-Science Reviews*, v. 12, p. 1–33. doi:10.1016/0012-8252(76)90052-0
- Sun, S.S., and McDonough, W.F., 1989, Chemical and isotopic systematics of oceanic basalts: implications for mantle composition and processes: *Geological Society Special Publications*, v. 42, no. 1, 313–345.
- Sun, W.D., Ding, X., Hu, Y.H., and Li, X.H., 2007, The golden transformation of the Cretaceous plate subduction in the west Pacific: *Earth and Planetary Science Letters*, v. 262, p. 533–542. doi:10.1016/j.epsl.2007.08.021
- Sun, W.D., Yang, X.Y., Fan, W.M., and Wu, F.Y., 2012, Mesozoic large scale magmatism and mineralization in South China: *Lithos*, v. 150, p. 1–5. doi:10.1016/j.lithos.2012.06.028
- Sun, Y., Ma, C.Q., Liu, Y.Y., and She, Z.B., 2011, Geochronological and geochemical constraints on the petrogenesis of Late Triassic aluminous A-type granites in southeast China: *Journal of Asian Earth Sciences*, v. 42, p. 1117–1131. doi:10.1016/j.jseaes.2011.06.007
- Sylvester, P.J., 1989, Post-collisional alkaline granites: *The Journal of Geology*, v. 97, p. 261–280.
- Wang, F.Y., Ling, M.X., Ding, X., Hu, Y.H., Zhou, J.B., Yang, X.Y., Liang, H.Y., Fan, W.M., and Sun, W.D., 2011, Mesozoic large magmatic events and mineralization in SE China: Oblique subduction of the Pacific plate: *International Geology Review*, v. 53, p. 704–726. doi:10.1080/00206814.2010.503736
- Wang, K., Sun, T., Chen, P., Ling, H., and Xiang, T., 2013b, The geochronological and geochemical constraints on the petrogenesis of the Early Mesozoic A-type granite and diabase in northwestern Fujian province: *Lithos*, v. 179, p. 364–381. doi:10.1016/j.lithos.2013.07.016
- Wang, L.J., Yu, J.H., Xu, X.S., Xie, L., Qiu, J.S., and Sun, T., 2007c, Formation age and origin of the Gutian-Xiaotao granitic complex in the southwestern Fujian province, China: *Acta Petrologica Sinica*, v. 23, p. 1470–1484.
- Wang, Q., Li, J.W., Jian, P., Zhao, Z.H., Xiong, X.L., Bao, Z.W., Xu, J. F., Li, C.F., and Ma, J.L., 2005b, Alkaline syenites in eastern Cathaysia (South China): Link to Permian-Triassic transtension: *Earth and Planetary Science Letters*, v. 230, p. 339–354.
- Wang, X.L., Zhou, J.C., Griffin, W.L., Zhao, G.C., Yu, J., Qiu, J.S., Zhang, Y.J., and Xing, G.F., 2014, Geochemical zonation across a Neoproterozoic orogenic belt: Isotopic evidence from granitoids and metasedimentary rocks of the Jiangnan orogen, China: *Precambrian Research*, v. 242, p. 154–171. doi:10.1016/j.precamres.2013.12.023
- Wang, Y., Fan, W., Cawood, P.A., Ji, S., Peng, T., and Chen, X., 2007b, Indosinian high-strain deformation for the Yunkaidashan tectonic belt, south China: Kinematics and (40)Ar/(39)Ar geochronological constraints: *Tectonics*, v. 26, p. TC6008. doi:10.1016/j.precamres.2013.12.027
- Wang, Y., Fan, W., Sun, M., Liang, X., Zhang, Y., and Peng, T., 2007a, Geochronological, geochemical and geothermal constraints on petrogenesis of the Indosinian peraluminous granites in the South China Block: A case study in the Hunan Province: *Lithos*, v. 96, p. 475–502. doi:10.1016/j.lithos.2006.11.010
- Wang, Y., Li, H., Fan, W., Liang, X., and Guo, F., 2002, U-Pb dating of early Mesozoic granodioritic intrusions in southeastern Hunan Province, South China and its petrogenetic implications: *Science in China (Series D:Earth Sciences)*, v. 45, p. 280–288. doi:10.1360/02yd9030
- Wang, Y.J., Fan, W.M., Liang, X.Q., Peng, T.P., and Shi, Y.R., 2005a, SHRIMP zircon U-Pb geochronology of Indosinian granites in Hunan Province and its petrogenetic implications: *Chinese Science Bulletin*, v. 50, p. 1395–1403. doi:10.1360/982004-603
- Wang, Y.J., Fan, W.M., Zhang, G.W., and Zhang, Y.H., 2013a, Phanerozoic tectonics of the South China Block: Key observations and controversy: *Gondwana Research*, v. 23, p. 1273–1305. doi:10.1016/j.gr.2012.02.019

- Wang, Y.J., Wu, C.M., Zhang, A.M., Fan, W.M., Zhang, Y.H., Zhang, Y.Z., Peng, T.P., and Yin, C.Q., 2012, Kwangsi and Indosinian reworking of the eastern South China Block: Constraints on zircon U–Pb geochronology and metamorphism of amphibolites and granulites: *Lithos*, v. 150, p. 227–242.
- Wang, Y.J., Zhang, Y.H., Fan, W.M., and Peng, T.P., 2005c, Structural signatures and ⁴⁰Ar/³⁹Ar geochronology of the Indosinian Xuefengshan tectonic belt, South China Block: *Journal of Structural Geology*, v. 27, p. 985–998. doi:10.1016/j.jsg.2005.04.004
- Whalen, J.B., Currie, K.L., and Chappell, B.W., 1987, A-type granites: Geochemical characteristics, discrimination and petrogenesis: *Contributions to Mineralogy and Petrology*, v. 95, p. 407–419. doi:10.1007/BF00402202
- Wu, Y., and Zheng, Y., 2013, Tectonic evolution of a composite collision orogen: An overview on the Qinling–Tongbai–Hong’an–Dabie–Sulu orogenic belt in central China: *Lithos*, v. 23, p. 1402–1428.
- Xiang, H., Zhang, L., Zhou, H.W., Zhong, Z.Q., Zeng, W., Liu, R., and Jin, S., 2008, U–Pb zircon geochronology and Hf isotope study of metamorphosed basic-ultrabasic rocks from metamorphic basement in southwestern Zhejiang: The response of the Cathaysia Block to Indosinian orogenic event: *Science in China Series D: Earth Sciences*, v. 51, p. 788–800. doi:10.1007/s11430-008-0053-0
- Xu, X., O Reilly, S.Y., Griffin, W.L., Wang, X., Pearson, N.J., and He, Z., 2007, The crust of Cathaysia: Age, assembly and reworking of two terranes: *Precambrian Research*, v. 158, p. 51–78. doi:10.1016/j.precamres.2007.04.010
- Yao, J., Shu, L., Santosh, M., and Li, J., 2015, Neoproterozoic arc-related andesite and orogeny-related unconformity in the eastern Jiangnan orogenic belt: Constraints on the assembly of the Yangtze and Cathaysia blocks in South China: *Precambrian Research*, v. 262, p. 84–100. doi:10.1016/j.precamres.2015.02.021
- Yao, J., Shu, L., Santosh, M., and Zhao, G., 2014, Neoproterozoic arc-related mafic–Ultramafic rocks and syn-collision granite from the western segment of the Jiangnan Orogen, South China: Constraints on the Neoproterozoic assembly of the Yangtze and Cathaysia Blocks: *Precambrian Research*, v. 243, p. 39–62. doi:10.1016/j.precamres.2013.12.027
- Yu, J.H., O Reilly, S.Y., Zhou, M.F., Griffin, W.L., and Wang, L.J., 2012, U–Pb geochronology and Hf–Nd isotopic geochemistry of the Badu Complex, Southeastern China: Implications for the Precambrian crustal evolution and paleogeography of the Cathaysia Block: *Precambrian Research*, v. 222–223, p. 424–449. doi:10.1016/j.precamres.2011.07.014
- Zhang, G.W., Guo, A.L., Wang, Y.J., Li, S.Z., Dong, Y.P., Liu, S.F., He, D. F., Cheng, S.Y., Lu, R.K., and Yao, A.P., 2013, Tectonics of South China continent and its implications: *Science China Earth Sciences*, v. 56, p. 1804–1828. doi:10.1007/s11430-013-4679-1
- Zhang, S.B., and Zheng, Y.F., 2013, Formation and evolution of Precambrian continental lithosphere in South China: *Gondwana Research*, v. 23, p. 1241–1260. doi:10.1016/j.gr.2012.09.005
- Zhang, Y.Q., Xu, X.B., Jia, D., and Shu, L.S., 2009, Deformation record of the change from Indosinian Collision-related tectonic system to yanshanian subduction-related tectonic system in South China during the early Mesozoic: *Earth Science Frontiers*, v. 16, p. 234–247. (in Chinese with English abstract).
- Zhao, G., 2015, Jiangnan Orogen in South China: Developing from divergent double subduction: *Gondwana Research*, v. 27, p. 1173–1180. doi:10.1016/j.gr.2014.09.004
- Zhao, G., and Cawood, P.A., 2012, Precambrian geology of China: *Precambrian Research*, v. 222–223, p. 13–54. doi:10.1016/j.precamres.2012.09.017
- Zhao, K., Jiang, S., Chen, W., Chen, P., and Ling, H., 2013, Zircon U–Pb chronology and elemental and Sr–Nd–Hf isotope geochemistry of two Triassic A-type granites in South China: Implication for petrogenesis and Indosinian trans-tensional tectonism: *Lithos*, v. 160–161, p. 292–306. doi:10.1016/j.lithos.2012.11.001
- Zhao, L., Guo, F., Fan, W., Li, C., Qin, X., and Li, H., 2012, Origin of the granulite enclaves in Indo-Sinian peraluminous granites, South China and its implication for crustal anatexis: *Lithos*, v. 150, p. 209–226. doi:10.1016/j.lithos.2012.02.015
- Zheng, Y., Wu, R., Wu, Y., Zhang, S., Yuan, H., and Wu, F., 2008, Rift melting of juvenile arc-derived crust: Geochemical evidence from Neoproterozoic volcanic and granitic rocks in the Jiangnan Orogen, South China: *Precambrian Research*, v. 163, p. 351–383. doi:10.1016/j.precamres.2008.01.004
- Zheng, Y.F., Xiao, W.J., and Zhao, G.C., 2013, Introduction to tectonics of China: *Gondwana Research*, v. 23, p. 1189–1206. doi:10.1016/j.gr.2012.10.001
- Zhou, X.M., Sun, T., Shen, W.Z., Shu, L.S., and Niu, Y.L., 2006, Petrogenesis of Mesozoic granitoids and volcanic rocks in South China: A response to tectonic evolution: *Episodes*, v. 29, p. 26–33.
- Zhu, K.Y., Li, Z.X., Xu, X.S., and Wilde, S.A., 2013, Late Triassic melting of a thickened crust in southeastern China: Evidence for flat-slab subduction of the Paleo-Pacific plate: *Journal of Asian Earth Sciences*, v. 74, p. 265–279. doi:10.1016/j.jseaes.2013.01.010
- Zhu, K.Y., Li, Z.X., Xu, X.S., and Wilde, S.A., 2014, A Mesozoic Andean-Type Orogenic Cycle in Southeastern China as Recorded by Granitoid Evolution: *American Journal of Science*, v. 314, p. 187–234. doi:10.2475/01.2014.06
- Zhu, K.Y., Li, Z.X., Xu, X.S., Wilde, S.A., and Chen, H.L., 2016, Early Mesozoic ferroan (A-type) and magnesian granitoids in eastern South China: Tracing the influence of flat-slab subduction at the western Pacific margin: *Lithos*, v. 240–243, p. 371–381. doi:10.1016/j.lithos.2015.11.025